Biochemical Engineering Journal 187 (2022) 108563

Contents lists available at ScienceDirect

Biochemical Engineering Journal

journal homepage: www.elsevier.com/locate/bej

Electrospun poly (Ɛ-caprolactone)-eggshell membrane nanofibrous mat as a potential wound dressing material

Mohammed Bello [a], Faizuan Abdullah [a,b,*], Wan Mohd Asyraf Wan Mahmood [a], Nik Ahmad Nizam Nik Malek [b], Khairunnadwa Jemon [c], Shafiquzzaman Siddiquee [d], Tan Yong Chee [a], Palanivel Sathishkumar [e,**]

[a] Department of Chemistry, Universiti Teknologi Malaysia, 81310 Skudai, Johor Bahru, Malaysia
[b] Centre for Sustainable Nanomaterials, Universiti Teknologi Malaysia, 81310 Skudai, Johor Bahru, Malaysia
[c] Department of Bioscience, Universiti Teknologi Malaysia, 81310 Skudai, Johor Bahru, Malaysia
[d] Institut Penyelidikan Bioteknologi, Universiti Malaysia Sabah, Kota Kinabalu, Sabah, Malaysia
[e] Green Lab, Department of Prosthodontics, Saveetha Dental College and Hospital, Saveetha Institute of Medical and Technical Sciences (SIMATS), Chennai 600 077, India

ARTICLE INFO

Keywords:
Antibacterial activity
Biocompatibility
Eggshell membrane
Electrospinning
Nanofibrous mat
Wound dressing material

ABSTRACT

Eggshell membrane (ESM) is a highly-collagenized, biopolymeric fibrous network generally considered domestic and industrial waste. However, its inherent extraordinary properties have made ESM widely used in different fields due to its high potential applications, especially in the biomedical field. In this study, a poly (Ɛ-caprolactone) (PCL) integrated ESM (PCL/ESM) nanofibrous mat is fabricated using an electrospinning technique to produce wound dressing materials with enhanced biocompatibility and antibacterial efficacy for potent tissue regeneration. The physicochemical, biological, and mechanical properties of the electrospun fabricated nanofibrous mat PCL (15% w/v) and PCL/ESM (0.5% w/v, 1.5% w/v, and 2.5% w/v) were investigated using FE-SEM, ATR-FTIR, DSC, and XRD. In addition, the water uptake ability, degradability, cell viability, and antibacterial activity of the mats were evaluated. The FTIR results revealed that the molecular interactions of ESM with the PCL are through hydrogen bond formation. The morphology and the nanofiber dimension of the electrospun fabricated mat are within the collagen dimensions present in the extracellular matrix. The overall results confirm that the PCL/ESM (2.5% w/v) have shown the most excellent mechanical properties with high biocompatibility and efficient antibacterial activity among the other fabricated mat. Therefore, this study suggests that electrospun PCL/ESM mat could be a potential material for wound dressing.

1. Introduction

Wound healing that is often not given sufficient medical attention in wound care management tends to become an intricate biological process, due to pathogenic infection by microbial organisms thereby prolonging the healing process [1,2]. A chronic non-healing wound is frequently susceptible to the bacterial infiltration and other microbial organisms that can interfere with the healing process by inducing prolonged chronic inflammation, disrupting the secretion of vital growth factors, and causing poor angiogenesis, resulting in critical conditions that may lead to the amputation of the affected portion of skin or even death [1,3]. Additionally, the approaches employed clinically do not seem to yield the desired expectations. Among them include the conventional/traditional method, which uses bandages, gauzes, and creams. They have since been implicated due to the limitations that include their inability to promote the reconstruction of the injured skin, their poor biocompatibility, and they require to be replaced so frequently [4]. Therefore, developing effective materials for potential wound dressing applications becomes imperative. Such dressing material should protect the wounds from bacterial inversions, have good biocompatibility, and promote wound healing [5–7]. Various woven and non-woven formulations were developed from natural and synthetic polymers [8–12]. Non-woven nanofibers that have been fabricated using the electrospinning technique have attracted the attention of most

* Corresponding author at: Department of Chemistry, Universiti Teknologi Malaysia, 81310 Skudai, Johor Bahru, Malaysia.
** Corresponding author.
E-mail addresses: faizuan@utm.my (F. Abdullah), salemsathishkumar@gmail.com (P. Sathishkumar).

https://doi.org/10.1016/j.bej.2022.108563
Received 9 February 2022; Received in revised form 22 July 2022; Accepted 24 July 2022
Available online 25 July 2022

researchers working in various biomedical fields, including wound dressing applications. And it could be due to their high porosity, large surface-area-to-volume ratio, and excellent mechanical and biological properties [13–16]. Hence, producing electrospun non-woven nanofibrous wound dressing materials containing antibacterial agents of natural sources is safer for potent wound healing applications [17].

Various formulations of antibacterial wound dressing materials have been developed from natural antibacterial agents that protect wounds against bacterial inversion and enhance cell adhesion, proliferation, migration, and differentiation, thereby; accelerating wound healing mechanisms [18]. The fabrication of ideal wound dressing biomaterial from poly (Ɛ-caprolactone) (PCL) and eggshell membrane (ESM) has been proposed due to their individual therapeutic properties [26]. For instance, PCL (an FDA-approved polymer) is a synthetic semicrystalline, biocompatible, biodegradable polymer possessing a functional ester bond that can be modified into a nontoxic topical pharmaceutical formulation that mimics the extracellular matrix (ECM) in chronic wounds [19]. Similarly, PCL has also been characterized by its flexibility, high plasticity, and slow degradation rate resulting from the hydrolysis of its ester bonds [20]. Despite its mimic ability of ECM, however, its inherent high hydrophobic capacity and poor hydrophilicity limit its use as a wound dressing material in biomedical applications and wound dressing applications [21].

Nevertheless, PCL has been widely used for its favorable mechanical properties, enhanced biocompatibility, sustained biodegradability, and ease of processibility with other polymers [22]. For instance, incorporating chitosan into PCL has been investigated by previous research using the electrospinning technique. Liverani et al. [23] have modified PCL electrospun nanofiber by incorporating bioactive glass particles in the blend of PCL and chitosan. The nanofiber composites demonstrated the potential as a bone tissue scaffold. Xu et al. [24] successfully fabricated a three-dimensional scaffold using polymer blend nanofiber consisting of cellulose acetate and PCL, which served as a binding agent. In another study, PCL enriched with nano chitosan (NC) nanofibrous mats were fabricated for curcumin delivery in wound healing [25]. The results revealed a remarkable increase in hydrophilicity, water uptake, and vapor transmission due to the incorporation of the NC in PCL. In addition, the curcumin-loaded PCL/NC exhibited excellent bioavailability, appropriate antibacterial activity, and sustained curcumin release behavior.

Millions of tons of eggshells produced by industry and households as waste have been overlooked, perhaps due to a lack of information on its inherent capabilities. ESM is known to be inexpensive, readily available, nontoxic, and environmentally benign. ESM is located between the eggshells and the albumen of an egg. ESM comprises more proteins, and the more significant portion of the proteins is primarily made up of collagens of type I, V, and X [26]. Other natural glycoproteins found in ESM and the collagens are glucosamine, hyaluronic acid, and chondroitin [27], which apply to the cutaneous wound healing application. ESM has also been documented to have an antibacterial property due to its ability to protect chronic wounds against bacterial inversions and promotes fibroblast cell proliferation and migration [28]. However, the network of disulfide bonds leads to its insolubility, thereby making its modification into various formulations a little more complicated. Despite this limitation, the incorporation of ESM into polymerous nanofibrous mats demonstrated nontoxicity and excellent mechanical property, which enhances its performance in various biomedical applications, including wound dressing [27]. For instance, Santos et al. [29] developed chitosan films by incorporating ESM powder (MCO) using the solvent evaporation method. The mechanical, chemical, biological, and thermal properties of the chitosan/MCO films, especially the composition with 10% MCO, exhibited better stability and more fit in biological systems. Nonetheless, a detailed study on PCL/ESM nanofiber mats of concentrations 0.5%, 1.5%, and 2.5%, dissolved in glacial acetic acid, produced using an electrospinning technique that demonstrates controllable biodegradation, excellent biocompatibility, and potent antibacterial property, and the suitable mechanical property was not yet reported in the literature. Therefore, the aim of this research was to fabricate PCL/ESM nanofiber mats with different concentrations of the ESM using the electrospinning technique. The physicochemical, mechanical, and thermal properties, water uptake measurement and degradation study as well as antibacterial activity and cell viability study of the electrospun nanofiber mats were assessed to determine their potentials as a wound dressing material.

2. Materials and methods

2.1. Materials

Poly (Ɛ-caprolactone) (PCL, Mw=80 K Da) was supplied by Sigma-Aldrich (MO, USA). ESM was purchased from Sinopharm Chemical Reagent Co. Ltd (Shanghai, China). Glacial acetic acid was purchased from QRëC (Johor Bahru, Malaysia), and the distilled water used was prepared in the Nanomaterial Laboratory (UTM, Malaysia).

2.2. Fabrication of electrospun PLC/ESM nanofibrous mats

Glacial acetic acid was used to prepare the 15% (w/v) PCL solutions. The solutions were stirred at 40 ^{o}C for 2 h to ensure the complete dissolution of the PCL. To prepare the PCL/ESM solutions, ESM powder was added to the PCL solutions to obtain 0.05 g, 0.15 g, and 0.25 g ESM per mL PLC/ESM solutions, which were equivalent to 0.5%, 1.5%, and 2.5% of PCL/ESM solutions, respectively. To ensure complete dispersion of the ESM in the PCL/ESM solutions, the solutions were continuously stirred at 40 ^{o}C for 4 h. 10 mL syringes with 18 G blunt-tip needles were used for the electrospinning of the mats. The electrospinning process was conducted at 20 kV applied voltage, 15 cm tip-to-collector distance, and the solution flow rate was 2 mL/h. The electrospun mats were collected on a static aluminium collector. The nanofibrous mats were dried in a vacuum at 37 ^{o}C for 24 h and used for further analysis.

2.3. Electrospun mat characterization

The morphological property of the nanofibrous mats was investigated by a field emission scanning microscope (FESEM, Carl Zeiss S.E., Singapore). The samples were sputter-coated with platinum using a sputtering device (JEOL, JFC 1200) before the FESEM analysis. The analysis was carried out at a probe current of 100 μA, a voltage of 5 kV, and a 30 μm aperture. ImageJ software (version 8.5) was used to analyze the FESEM micrographs to determine the average diameter of the nanofibrous mats. An average of 50 counts was taken from each micrograph.

The functional properties of the fabricated nanofibrous mats were investigated with a Fourier transform infrared spectroscope (Perkin Elmer FTIR spectrometer, Waltham, USA), fitted with attenuated total reflectance (ATR). The ATR spectra were recorded within 4000–650 cm^{-1} with a resolution of 8 cm^{-1}.

The DSC measurements were carried out on the electrospun nanofibrous mats using Q10 DSC (Mettler Toledo DSC 822e, Greifensee, Switzerland). The heating of the mats was performed within the range of − 40–400 ^{o}C, at a heating rate of 10 ^{o}C/min, and a flow rate of Nitrogen at 10 mL/min. The melting temperature of the mats was determined from the respective curves. X-ray diffractometer, Rigaku Corp. (XRD, Tokyo, Japan) was used to determine the crystallinity of the electrospun nanofibrous mats. The method employed in this work was reported elsewhere [30]. Typically, the Cu/Kα radiation was used at wavelength 1.54 Å. The current used was 15 mA at the voltage of 30 kV, and the analysis was conducted within the 5^{o} to 80^{o} angle range. The pattern of nanofibrous mats diffraction was recorded and analyzed.

The universal testing machine Shimadzu Autograph, AG-Xplus series, was used to test the mechanical properties of PCL and PCL/ESM nanofibrous mats. The standard ASTM D3039 method was used to

evaluate the mats. Samples were cut into a rectangular shape of 50 × 10 mm. The two ends of the samples were fixed on the two grips of the machine, and a 500 N load was applied at the rate of 5 mm/min with a 30 mm gauze length. A digital vernier caliper was used to measure the thickness of the mats from 5 random positions before the mechanical testing.

2.4. Water uptake measurement

The water uptake (body fluid uptake) of the PCL and PCL/ESM nanofibrous mats was determined by incubating each of the mats in PBS (pH 7.4), set at 37 °C for a predetermined time. Typically, about 10 mg of each nanofibrous mat (W_1) was immersed in 20 mL of PBS for a specified duration. At an interval of 2 h, 4 h, 6 h, 24 h, 48 h, and 72 h, each mat was removed from the medium and blotted with filter paper to clean the excess PBS before weighing (W_2) again. The percentage of water uptake was calculated using Eq. (1) as follows:

$$Water\quad uptake(\%) = \frac{(W_2 - W_1)}{W_1} \times 100 \tag{1}$$

2.5. Degradability study

The degradation study of the PCL and its composite mats was determined according to the method reported previously [26], with slight modification. Briefly, each sample was cut in 1 × 1 cm size and allowed to dry in an oven set at 40 °C for 24 h before weighing (W_0). The dried mats were submerged in PBS of pH 7.4 and incubated at 37 °C for a specified period. At a predetermined time interval, each of the mats was removed from the medium, and ultra-distilled water was used to wash off the PBS and dry it at room temperature before it was weighed (W_t) again. The percentage weight loss of each of the samples was calculated using Eq. (2) as follows:

$$Weight\quad loss(\%) = \frac{(W_0 - W_t)}{W_0} \times 100 \tag{2}$$

2.6. Cell viability test

The metabolic activity of the seeded L929 mouse fibroblast cells was studied to determine the percentage cell viability (cytotoxicity) of the electrospun PCL, PCL/ESM nanofibrous mats according to the ISO 10993–5 standard method [31]. Typically, the samples were immersed in 75% ethanol. After about 30 min sterilization, the samples were removed and washed with PBS. A 24-well tissue culture plate was used to culture 1 mL suspension of L929 cells with a 1×10^6 cell/well density in CDMEM. The culture plates were incubated in a 5% CO_2 incubator set at 37 °C for 24 h. After 24 h, a fresh CDMEM was used to replace the old one, and 1 mg of each sample was placed in each well. The plates were then incubated again in 5% CO_2 set at 37 °C for 24 h and 72 h. After completing the 24 h and 72 h incubation, the samples in the old media were removed, and each well was washed with 0.5 mL of PBS solution. Each well that contained the media was replaced with 770 μL MTT solution (0.5 mg/mL), covered with aluminium foil, and the plates were then incubated again at the same temperature (37 °C) for 3 h. After the incubation, a Formazan crystal formed in each well was dissolved by adding 350 μL of dimethyl sulphoxide (DMSO). A 200 μL of the solution from each well was transferred into a 96 well plate. The optical density of the samples was measured at 540 nm using an ELISA reader. The percent viability of each of the nanofibrous mats was calculated using Eq. (3), n = 6, as follows [32]:

$$Viability\quad (\%) = \frac{A_{test}}{A_{control}} \times 100 \tag{3}$$

where, A_{test} represents absorbance of the cells treated with the sample, and $A_{control}$ is absorbance of the cells without sample.

2.7. Antibacterial activity test

The antibacterial activity of the electrospun PCL and PCL/ESM nanofibrous mats was evaluated based on the work reported by Adeli et al. [31]. The samples were assessed against gram-positive *Staphylococcus aureus* (ATCC 6538) and gram-negative *Escherichia coli* (ATCC 11229) bacterial strains. The mats were cut into a 10 × 10 mm shape and were sterilized by submerging them in 75% ethanol for about 30 min, rinsed with PBS, and finally, dried under convection air and UV light. Each sample was then immersed into a bacterial suspension (1.5×10^6 CFU/mL) and was moved into an incubator-shaker set at 100 rpm, 37 °C, and cultivated after 24 h. Subsequently, 200 μL of each treated bacterial solution was serially diluted, and a drop-plate method was used to determine the number of viable bacteria. The fabricated mat's antibacterial efficiency (R) was determined by calculating the % Reduction of the bacterial cells (n = 3) using Eq. (4) [33]:

$$R(\%) = \frac{CFU_{(control)} - CFU_{(sample)}}{CFU_{(control)}} \times 100 \tag{4}$$

3. Results and discussion

3.1. Electrospun mat characterization

3.1.1. FESEM analysis

In the present research, the electrospun PCL, ESM, and PCL/ESM nanofibrous mats of various concentrations were successfully fabricated using the electrospinning technique. The morphology of the nanofibrous mats was characterized by FESEM analysis, as shown in Fig. 1, which confirmed the formation of the composite in uniformed, and bead-free nanofibers. The FESEM micrographs with their respecting average nanofiber diameter distributions are illustrated in Fig. 1, while the various average diameters according to different concentrations are shown in Table 1. The images of the nanofiber mats have evinced randomly oriented, smooth, and beads-free mats with a mean diameter of 111 ± 15 nm to 156 ± 29 nm. The mean diameter of pristine PCL and PCL/ESM (0.5% w/v) was found to be 128 ± 23 nm and 111 ± 15 nm, respectively. A clear difference has been observed, perhaps, due to the decrease in viscosity of the electrospinning solutions, following the loading of ESM. However, PCL/ESM (1.5% w/v) and PCL/ESM (2.5% w/v) nanofibrous mats have increased their average nanofiber diameter of 124 ± 21 nm and 156 ± 29 nm, respectively. The changes in the average nanofiber diameter could be due to the increased viscosity of their respective solutions. The nanofibre's morphology and dimensions are within the collagen dimensions present in the extracellular matrix (10–300 nm), and such a mat will promote human dermal fibroblast growth [25].

3.1.2. ATR-FTIR analysis

The formation of composite PCL nanofibrous mat with ESM was evaluated by ATR-FTIR spectra to determine the chemical composition of the matrices. Fig. 2 shows the transmission spectra of pristine PCL, ESM, and PCL/ESM (0.5% w/v, 1.5% w/v, and 2.5% w/v) nanofibrous mats of varying concentrations. The pristine PCL structure has a typical carbonyl stretching peak at 1723 cm^{-1} (C═O stretch). The characteristic peaks around 2944 cm^{-1} and 2867 cm^{-1} are attributed to asymmetrical and symmetrical stretching of C-H (CH_2 stretch), respectively [34,35]. The absorption bands at 1294 cm^{-1} and 1239 cm^{-1} are due to C-C and C-O stretching. Similarly, the amorphous phase's absorption bands between 1178 cm^{-1} and 1165 cm^{-1} correspond to C-O-C stretching, C-O, and C-C stretching [25]. However, in two specific regions, the ESM spectrum in Fig. 2 indicates the characteristic absorption bands attributed to collagen (type I, V, and X) functional groups. The regions are at 3750–2500 cm^{-1} and the regions below 1700 cm^{-1} [36]. The characteristic peaks that appeared at 2944 cm^{-1} are due to asymmetric stretching vibrations of C-H bonds present in =CH_2 and =C-H groups [36]. The

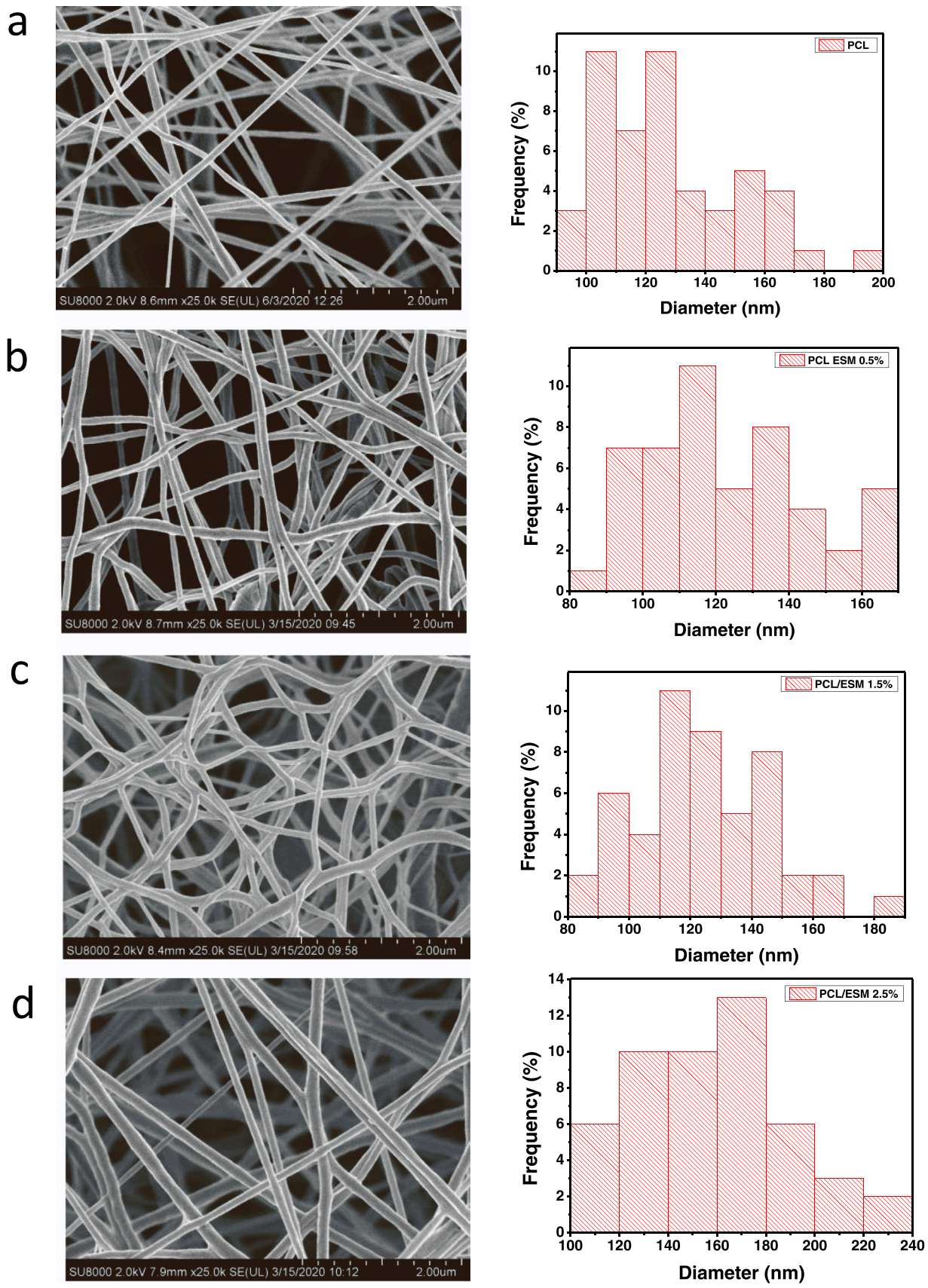

Fig. 1. FESEM images with the corresponding average fiber diameter distributions of (a) PCL, (b) PCL/ESM 0.5% w/v, (c) PCL/ESM 1.5% w/v, and (d) PCL/ESM 2.5% w/v.

Table 1
Size of the electrospun fabricated PCL and PCL/ESM nanofibers.

Sample code	Electrospun mats	ESM content	Average diameter of nanofibers
S1	PCL	0% w/v	128±23 nm
S2	PCL/ESM	0.5% w/v	111±15 nm
S3	PCL/ESM	1.5% w/v	124±21 nm
S4	PCL/ESM	2.5% w/v	156±29 nm

Diameter of nanofibers is mean ± SD, n=50.

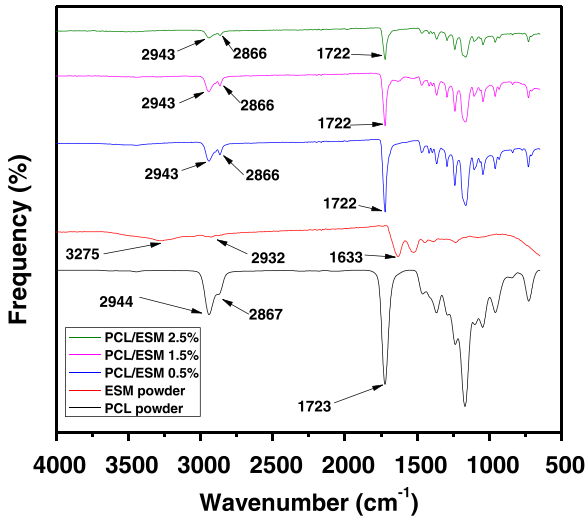

Fig. 2. ATR-FTIR spectra of electrospun PCL 15% w/v, ESM powder, PCL/ESM 0.5% w/v, PCL/ESM 1.5% w/v, and PCL/ESM 2.5% w/v.

most intensive absorption band exhibited at 3275 cm^{-1} is associated with stretching vibrations of O-H and N-H groups [37]. The peaks appeared at 1633 cm^{-1} (C═O stretching), 1525 cm^{-1} (C-N stretching/NH bending modes), and 1234 cm^{-1} (C-N stretching) are associated with amide I, amide II, and amide III of the glycoprotein fibers, respectively [38]. Furthermore, the peaks at 1446 cm^{-1}, 1075 cm^{-1}, and 620 cm^{-1} correspond to the CH_2 scissoring, amine (C-N stretching), and C-S stretching modes [36]. Nevertheless, the characteristic peaks of the PCL/ESM nanofibrous mats spectra are illustrated in Fig. 2. Broadband between 3750 cm^{-1} and 2500 cm^{-1} was observed in the PCL/ESM (0.5%) nanofibrous mat, which can be attributed to O-H/N-H stretch due to inter and intramolecular hydrogen bond formation [39]. The major bands of both the PCL and ESM were observed in the PCL/ESM (0.5% w/v, 1.5% w/v, and 2.5% w/v) nanofibrous mats; those bands of ESM were shifted and superimposed by the bands of the PCL. For instance, the peaks associated with C═O stretch at 1633 cm^{-1} and 1723 cm^{-1} in ESM and PCL spectra, respectively, were shifted to 1722 cm^{-1} in PCL/ESM (0.5% w/v, 1.5% w/v, and 2.5% w/v) nanofibrous mats spectra. Similarly, the asymmetric C-H stretching vibration at 2932 cm^{-1} in the ESM spectrum was shifted to 2943 cm^{-1} in the composites. This affirms that there was an interaction between the PCL and the ESM. It was also observed that the peak intensities of the broadband associated with O-H/N-H, the asymmetric and symmetric C-H stretch had been reduced in the PCL/ESM nanofibrous mats as the concentration of the ESM increased in the electrospinning solutions. The changes in peak intensities and the shifting of some characteristic peaks indicate that PCL and ESM are bound together.

3.1.3. DSC analysis

The DSC thermograms of the fabricated nanofibrous mats PCL and PCL/ESM (0.5% w/v, 1.5% w/v, and 2.5% w/v) were investigated, as shown in Fig. 3. The DSC profile of the pristine PCL has demonstrated a

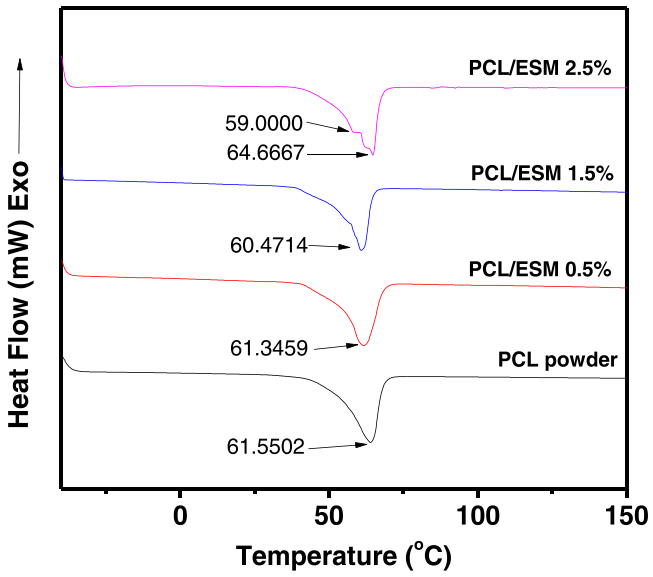

Fig. 3. DSC thermographs of PCL powder, PCL/ESM 0.5% w/v, PCL/ESM 1.5% w/v, and PCL/ESM 2.5% w/v.

sharp melting endotherm peak at 61.55 °C. However, with the loading of 0.5% ESM to the PCL solution, the melting endotherm peak of the PCL/ESM (0.5%) nanofibrous mat was slightly shifted to a lower temperature, confirming that it was the presence of the ESM that led to the change in the peak position of the pristine PCL. The loading of higher concentrations of 1.5% and 2.5% ESM have evinced the continued shift to lower temperatures of 60.47 °C and 59.00 °C, respectively, and subsequently shifted to 64.67 °C in the case of PCL/ESM (2.5%) nanofibrous mat where the two peaks share the same base. The melting temperature shift from the lower to the higher melting point could be due to incomplete melting of the composite at the lower temperature (59.00 °C). The PCL/ESM (2.5%) nanofibrous mat had to complete its melting point at 64.66 °C. Therefore, the shifting of the peak positions could be attributed to the formation of hydrogen bonds between the pristine PCL and the ESM. The ATR-FTIR results have confirmed the fine dispersion of ESM over the mats. These results were consistent with the previous report of Santos et al. [29].

3.1.4. XRD analysis

The molecular interactions in the various nanofibrous mats were further investigated by XRD analysis. The XRD profile of PCL and ESM were presented in Fig. 4(a). The XRD profile of pristine PCL shows characteristic sharp peaks at $2\theta = 21.3^{o}$ and 23.8^{o}, as reported by Trakoolwannachai et al. [40], and they represent (102) and (014) reflection planes. These peaks were matched with the JCPDS 96–411–7252 card. Similarly, the diffractogram of ESM presented peaks of semicrystalline dispersion with a broad base between $2\theta = 10^{o} - 30^{o}$, with the highest intensity peak at $2\theta = 21.1^{o}$ representing a (21−1) reflection plane as contained in JCPDS 96–200–9704 card. The X-ray diffractogram of PCL/ESM (0.5%, 1.5%, and 2.5% w/v) nanofibrous mats are presented in Fig. 4(b). The characteristic peaks of PCL in the nanofibrous mats were slightly shifted at $2\theta = 21.4^{o}$ and 23.7^{o}, representing (102) and (014) reflection planes, respectively. Indeed, the increase in ESM concentration had resulted in some changes in crystallinity of the PCL and the PCL/ESM (0.5% w/v) nanofibrous mats. And also, a similar change has been observed between the PCL/ESM (0.5% w/v) and PCL/ESM (2.5% w/v) (Fig. 4b). These changes in the characteristic peaks of PCL could be due to the amorphous nature of the ESM powder in the matrices. This affirms that PCL's orientation and crystal structure in the PCL/ESM had changed. The present research results confirm the molecular interactions of the PCL and ESM, as illustrated in the ATR-FTIR

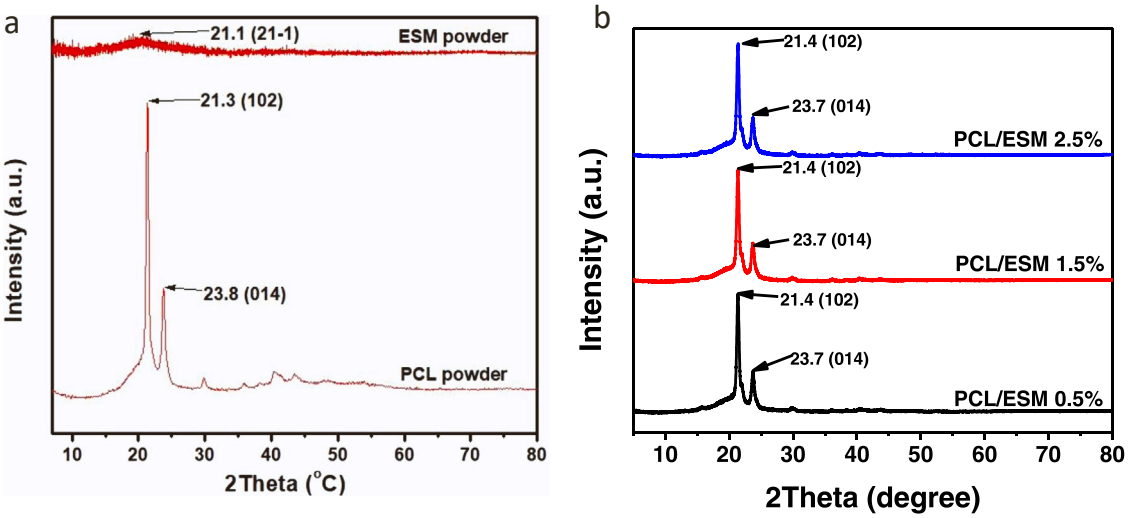

Fig. 4. XRD patterns of (a) pristine PCL and pristine ESM, and (b) PCL/ESM nanofibrous mats of different ESM concentrations with their corresponding crystallinity.

and DSC results, and they agree with the work of Trakoolwannachai et al. [40].

3.1.5. Mechanical testing

The mechanical properties of the nanofibrous mat are also considered another important parameter for biomedical applications and wound dressing applications. Table 2 presents the mean values of tensile strength, elongation at break, and Young's modulus of the PCL and PCL/ESM (0.5% w/v, 1.5% w/v, 2.5% w/v) nanofibrous mats. As shown in Table 2, pristine PCL presented adequate tensile strength, confirming its high mechanical properties, while ESM is already known for its weak mechanical strength. As a result, the blending of PCL with ESM powder can overcome the ESM's poor mechanical properties by achieving some amount of strength. Table 2 shows that the increase in ESM concentration from 0.5% (w/v) to 2.5% (w/v) in the PCL mats increases the tensile strength, and Young's modulus of the PCL/ESM nanofibrous mats. The tensile strength of the PCL/ESM (0.5% w/v, 1.5% w/v, and 2.5% w/v) nanofibrous mats was found to be 3.06 MPa, 3.15 MPa, and 4.12 MPa can withstand the strain of 79.65%, 64.55%, and 55.73%, respectively. The results revealed that incorporating ESM powder into PCL mats improved the mechanical behavior of PCL/ESM nanofibrous mats [41]. It can be ascribed that PCL/ESM 2.5% demonstrates the highest tensile strength and can be suitable for biomedical and wound dressing applications, considering its tensile strength has fall within the bench mark 0.5 – 16 MPa for use in biomedical and wound dressing applications [25]. This result concludes that the mechanical strength of a drug-loaded PCL/ESM nanofibrous mat can be a possible candidate for wound dressing application.

3.2. Water uptake measurement

The water uptake property is an important parameter that demonstrates the biocompatibility nature of biodegradable nanofibrous mats. It demonstrated that the water uptake capacity of pristine PCL nanofibrous mat reached saturation at 24 h (158%) and then began to decrease to lower capacity. It decreased to 147% after 72 h. The low water uptake demonstrated by the pristine PCL could be attributed to its hydrophobic property. The results have shown a dramatic increase in the water uptake by adding eggshells to the polymer matrix. The water uptake capacity increased to 180% and 208% at 72 h, after the addition of 0.5% (w/v) and 2.5% (w/v) ESM, respectively. The increase in the water uptake ability can be associated with the decrease in the hydrophobicity of the mats. In other words, the hydrophilicity of the mats has considerably increased. Nevertheless, PCL/ESM (2.5% w/v) nanofibrous mat had the highest water uptake capacity at 210%, as shown in Fig. 5a.

Table 2
Properties of the electrospun fabricated PCL and PCL/ESM mats.

Electrospun mats	Tensile strength (MPa)	Elongation at brake (%)	Young's Modulus (MPa)
PCL	5.18±1.69	100.29±2.56	8.73±1.72
PCL/ESM 0.5%	3.06±1.67	79.65±2.03	10.51±1.12
PCL/ESM 1.5%	3.15±0.96	64.55±1.97	12.56±1.51
PCL/ESM 2.5%	4.12±0.75	55.73±2.31	14.31±1.71

Tensile strength, Elongation at brake and the Young's modulus are mean ± SD, n=5.

3.3. Degradation study

After seven and fourteen days, the degradation study of PCL and PCL/ESM nanofibrous mat (0.5% w/v, 1.5% w/v, and 2.5% w/v) was illustrated in Fig. 5b. After 14 days of degradation of the pristine PCL and that of the PCL/ESM mats, both the PCL and its composite have exhibited degradation due to their loss of weight. The pristine PCL exhibited the least morphological change, possibly due to its hydrophobic nature. The degradation of the PCL occurred mostly at the surface of the mat following the inability of the medium to easily infiltrate the polymeric matrix [25]. However, the incorporation of ESM into PCL has enhanced the degree of degradation. On day seven, pristine PCL was reduced to 98.61% and PCL/ESM 2.5%, 95.02%. Accordingly, on day 14, PCL/ESM 2.5% exhibited the highest weight loss to 86.84% compared to the other mats. The results of this research were consistent with the previous report [25].

3.4. Cell viability

An ideal wound dressing material is also expected to be suitable for biocompatibility. MTT assay was used according to ISO 10993–5 standard to determine the percent cell viability of the PCL/ESM (0.5% w/v, 1.5% w/v, and 2.5% w/v) nanofibrous mats. In this research, the in vitro MTT assay allowed the L929 fibroblast cells to be cultured with the extract medium of PCL/ESM nanofibrous mats for 24 h (Day1) and 72 h (Day3). The L929 cells were able to form a purple formazan crystal. As illustrated in Fig. 6a, the results showed remarkable cell viability above 90% for the tested mats after 24 h (Day1) and 72 h (Day3) of contact with the fibroblast cells. According to the ISO 10993–5 standard, any mat that exhibits less than 70% cell viability is equivalent to being cytotoxic and cannot be considered a biomaterial used in biomedical applications and wound dressing applications [2]. The control which

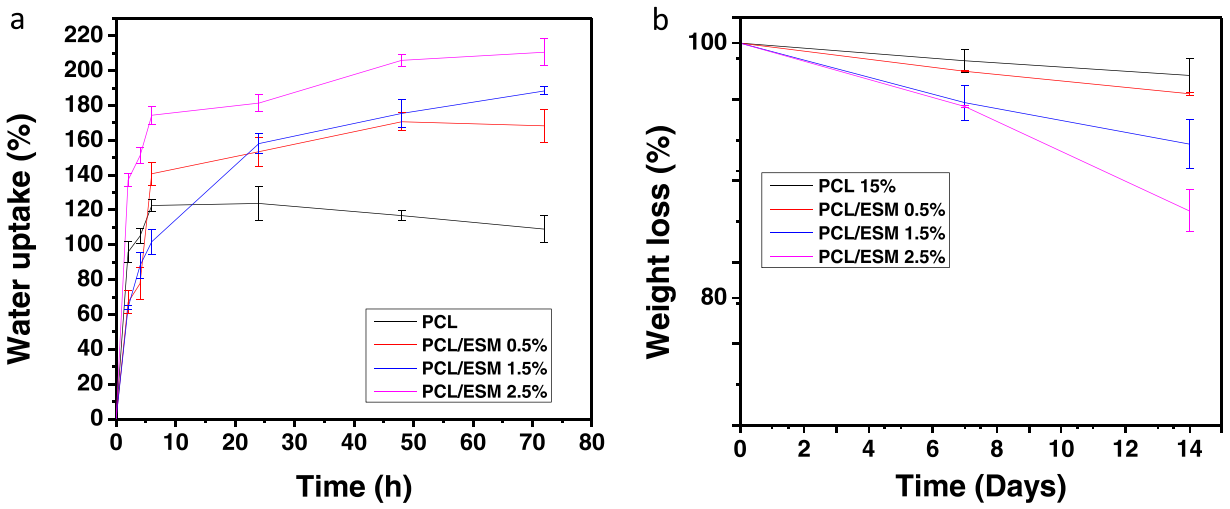

Fig. 5. (a) Water uptake capacities (b) in vitro biodegradability of pristine PCL, PCL/ESM 0.5% (w/v), PCL/ESM 1.5% (w/v), and PCL/ESM 2.5% (w/v).

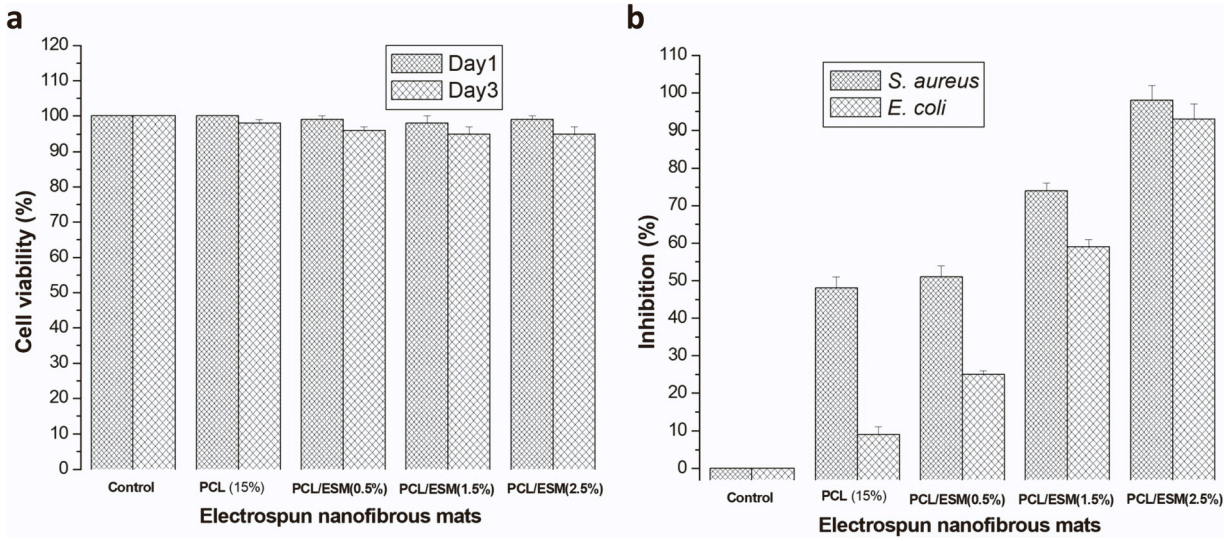

Fig. 6. (a) Cytotoxicity and (b) antibacterial activity assessment of the fabricated electrospun mats.

contained the inoculated solution without a nanofiber mat demonstrates 100% viable cells. After one day of incubation, PCL nanofibrous mats have demonstrated cell viability 110.62 ± 3.94%, whereas PCL/ESM 0.5% mat elucidated a high cells viability of 121.99 ± 1.63%. The results revealed that the incorporation of ESM into the PCL matrix had caused the increased in cells viability in PCL/ESM 0.5% nanofibrous mats. A similar impact of ESM on a hybrid polymer of CS/PCL has been reported in the work of Guha et al. [43].

3.5. *In vitro antibacterial activity test*

A colony count method was used to evaluate the antibacterial efficacy of the electrospun PCL and PCL/ESM nanofibrous mats by determining the percent growth reduction against the bacterial strains of both the gram-positive *S. aureus*, and gram-negative *E. coli*, due to their interaction with the as-prepared electrospun nanofibrous mats. Fig. 6b shows the results of the control sample's antibacterial activity (% inhibition) (untreated cultured bacterial solution), pristine PCL, and electrospun PCL/ESM nanofibrous mats containing different concentrations of the ESM as against the bacterial strains. The results demonstrate the increase in antibacterial activity against both the *S. aureus* and the *E. coli* as ESM concentration increased. As shown in Fig. 6b, the antibacterial activity against *S. aureus* increased from 48% to 51%, 74%, and 98% in comparison with that against *E. coli* in which the antibacterial activity was increased from 9% to 25%, 59%, and 93% for 0.5%, 1.5%, and 2.5% for ESM-loaded PCL mat. Additionally, no inhibition was demonstrated by the control. These results indicate that the presence of NH^{3+} in ESM may have led to some metabolic changes, consequently resulting in inhibiting bacterial growth [25]. An increase in the antibacterial activity was shown after the increase of ESM to the pristine PCL solution, exhibiting the antibacterial activity of ESM distinctly. This behavior of ESM was in agreement with the previous report of Li et al. [42]. The same trend was demonstrated by PCL and PCL/ESM nanofiber mats against gram-negative *E. coli*. The results indicate that the concentration of ESM in PCL/ESM 0.5% (w/v) was not enough to inhibit the growth *of E. coli* bacteria. This could be due to the nature of the cellular wall around the *E. coli* bacteria, which gave it additional protection. However, as the concentration of the ESM increased in the mat, the antibacterial efficacy prevailed. The results, therefore, ascribed PCL/ESM 2.5% nanofibrous mats with excellent antibacterial activity to be a promising antibacterial wound dressing material.

4. Conclusions

In this study, poly (Ɛ-caprolactone) nanofibrous mats were successfully modified with eggshell mats using an electrospinning technique to produce wound dressing materials with improved biocompatibility and antibacterial efficiency for potent tissue regeneration. The study results revealed the molecular interactions of the ESM with the PCL through hydrogen bond formation. The morphology and the fiber dimension of the samples are within the collagen dimensions present in the extracellular matrix (10–300 nm) [25]. The samples, especially PCL/ESM 2.5% (w/v), have demonstrated optimal biocompatibility, no cytotoxicity, antibacterial efficacy, and good mechanical properties. Therefore, incorporating the 2.5% concentration of ESM into PCL has shown its great potential for use as wound dressing material. However, it is recommended that the PCL/ESM 2.5% nanofibrous mats be evaluated for their drug release ability and their in vitro and in vivo wound healing efficacies.

CRediT authorship contribution statement

Mohammed Bello: Conceptualization, Sampling, Investigation, Methodology, Formal analysis, Writing – original draft. **Faizuan Abdullah**: Conceptualization, Funding, Validation, Writing – review & editing. **Wan Mohd Asyraf Wan Mahmood**: Writing – review & editing. **Nik Ahmad Nizam Nik Malek**: Writing – review & editing. **Khairunnadwa Jemon**: Writing – review & editing. **Shafiquzzaman Siddiquee**: Writing – review & editing. **Tan Yong Chee**: Writing – review & editing. **Palanivel Sathishkumar**: Methodology, Writing – review & editing.

Declaration of Competing Interest

The authors declare that they have no known competing financial interests or personal relationships that could have appeared to influence the work reported in this paper.

Data Availability

Data will be made available on request.

Acknowledgment

The research was supported by grants from Universiti Teknologi Malaysia (UTM) and the Ministry of Higher Education, Malaysia, with Vote Nos. Q. J130000.2509.20H51 and R.J130000.7854.5F115. I also appreciate my Nigerian Government for the support I received from the Tertiary Education Trust Fund (TETFUND) through the College of Education, Zing, Taraba State, by allowing me to pursue a Ph.D. degree in Malaysia.

References

[1] R. Ahmed, M. Tariq, I. Ali, R. Asghar, P. Noorunnisa Khanam, R. Augustine, A. Hasan, Novel electrospun chitosan/polyvinyl alcohol/zinc oxide nanofibrous mats with antibacterial and antioxidant properties for diabetic wound healing, Int. J. Biol. Macromol. 120 (2018) 385–393.

[2] M. Maaz Arif, S.M. Khan, N. Gull, T.A. Tabish, S. Zia, R. Ullah Khan, S.M. Awais, M. Arif Butt, Polymer-based biomaterials for chronic wound management: Promises and challenges, Int. J. Pharm. 598 (2021), 120270.

[3] D.C. Aduba Jr, S.S. An, G.S. Selders, W.A. Yeudall, G.L. Bowlin, T. Kitten, et al., Electrospun gelatin-arabinoxylan ferulate composite fibers for diabetic chronic wound dressing application, Int. J. Polym. Mater. 68 (2019) 660–668.

[4] S.P. Miguel, D.R. Figueira, D. Simões, M.P. Ribeiro, P. Coutinho, P. Ferreira, I. J. Correia, Electrospun polymeric nanofibres as wound dressings: a review, Colloids Surf. B 169 (2018) 60–71.

[5] H. Liu, C. Wang, C. Li, Y. Qin, Z. Wang, F. Yang, Z. Li, J. Wang, A functional chitosan-based hydrogel as a wound dressing and drug delivery system in the treatment of wound healing, RSC Adv. 8 (2018) 7533–7549.

[6] J. Lu, Y. Chen, M. Ding, X. Fan, J. Hu, Y. Chen, J. Li, Z. Li, W. Liu, A 4arm-PEG macromolecule crosslinked chitosan hydrogels as antibacterial wound dressing, Carbohydr. Polym. 277 (2022), 118871.

[7] S. Zhang, Z.Y. Yang, J. Hao, F. Ding, Z. Li, X. Ren, Hollow nanosphere-doped bacterial cellulose and polypropylene wound dressings: biomimetic nanocatalyst mediated antibacterial therapy, Chem. Eng. J. 432 (2022), 134309.

[8] A.D. Badaraev, A. Koniaeva, S. Krikova, E.V. Shesterikov, E.N. Bolbasov, A. L. Nemoykina, V.M. Bouznik, K.S. Stankevich, Y.M. Zhukov, I.P. Mishin, E. Varakuta, S.I. Tverdokhlebov, Piezoelectric polymer membranes with thin antibacterial coating for the regeneration of oral mucosa, Appl. Surf. Sci. 504 (2020), 144068.

[9] J. Chen, C. Kuo, W. Lee, Thermo-responsive wound dressings by grafting chitosan and poly(N-isopropylacrylamide) to plasma-induced graft polymerization modified non-woven fabrics, Appl. Surf. Sci. 262 (2012) 95–101.

[10] D. Marković, H. Tseng, T.S. Nunney, M. Radoičić, T. Ilic-Tomic, M. Radetić, Novel antimicrobial nanocomposite based on polypropylene non-woven fabric, biopolymer alginate and copper oxides nanoparticles, Appl. Surf. Sci. 527 (2020), 146829.

[11] M.J. Jasni, M. Arulkumar, P. Sathishkumar, A.R. Mohd Yusoff, N.A. Buang, F.L. Gu, Electrospun nylon 6,6 membrane as a reusable nano-adsorbent for bisphenol A removal: Adsorption performance and mechanism, J. Colloid Interface Sci. 508 (2017) 591–602.

[12] A.M. Zahari, C. Shuo, P. Sathishkumar, A.R. Mohd Yusoff, F.L. Xu, N.A. Buang, W. J. Lau, R.J. Gohari, Z. Yusop, A reusable electrospun PVDF-PVP-MnO2 nanocomposite membrane for bisphenol A removal from drinking water, J. Environ. Chem. Eng. 6 (2018) 5801–5811.

[13] S. Fahimirad, H. Abtahi, P. Satie, E. Ghaznavi-Rad, M. Moslehi, A. Ganji, Wound healing performance of PCL/chitosan-based electrospun nanofiber electrosprayed with curcumin loaded chitosan nanoparticles, Carbohydr. Polym. 259 (2021), 117640.

[14] S.N. Kalva, R. Augustine, A.A. Mamun, Y.B. Dalvi, N. Vijay, A. Hasan, Active agents loaded extracellular matrix mimetic electrospun membranes for wound healing applications, J. Drug Deliv. Sci. Technol. 63 (2021), 102500.

[15] S. Thenmozhi, N. Dharmaraj, K. Kadirvelu, H.Y. Kim, Electrospun nanofibers: New generation materials for advanced applications, Mater. Sci. Eng. B 217 (2017) 36–48.

[16] L. Bacakova, M. Zikmundova, J. Pajorova, A. Broz, E. Filova, A. Blanquer, et al., Nanofibrous scaffolds for skin tissue engineering and wound healing based on synthetic polymers. Applied Nanobiotechnology, IntechOpen, 2019.

[17] A.D. Juncos Bombin, N.J. Dunne, H.O. McCarthy, Electrospinning of natural polymers for the production of nanofibres for wound healing applications, Mater. Sci. Eng. C. 114 (2020), 110994.

[18] J. Avossa, G. Pota, G. Vitiello, A. Macagnano, A. Zanfardino, M. Di Napoli, A. Pezzella, G. D'Errico, M. Varcamonti, G. Luciani, Multifunctional mats by antimicrobial nanoparticles decoration for bioinspired smart wound dressing solutions, Mater. Sci. Eng. C 123 (2021), 111954.

[19] P.A. Maroju, P. Tata, A. Balapure, J.R. Dutta, R. Ganesan, *Lactobacillus amylovorus* derived lipase-mediated silver derivatization over poly(ε-caprolactone) towards antimicrobial coatings, Enzym. Microb. Technol. 150 (2021), 109888.

[20] S.R. Gomes, G. Rodrigues, G.G. Martins, M.A. Roberto, M. Mafra, C.M. Henriques, J.C. Silva, In vitro and in vivo evaluation of electrospun nanofibers of PCL, chitosan and gelatin:a comparative study, Mater. Sci. Eng. C 46 (2015) 348–358.

[21] A. Sadeghianmaryan, Z. Yazdanpanah, Y.A. Soltani, H.A. Sardroud, M. H. Nasirtabrizi, X.C. Chen, Curcumin-loaded electrospun polycaprolactone/montmorillonite nanocomposite: wound dressing application with antibacterial and low cell toxicity properties, J. Biomater. Sci. Polym. Ed. 31 (2020) 169–187.

[22] J. Wang, M. Windbergs, Functional electrospun fibers for the treatment of human skin wounds, Eur. J. Pharm. Biopharm. 119 (2017) 283–299.

[23] L. Liverani, J. Lacina, J.A. Roether, E. Boccardi, M.S. Killian, P. Schmuki, D. W. Schubert, A.R. Boccaccini, Incorporation of bioactive glass nanoparticles in electrospun PCL/chitosan fibers by using benign solvents, Bioact. Mater. 3 (2018) 55–63.

[24] T. Xu, Z. Liang, B. Ding, Q. Feng, H. Fong, Polymer blend nanofibers containing polycaprolactone as biocompatible and biodegradable binding agent to fabricate electrospun three-dimensional scaffolds/structures, Polymers 151 (2018) 299–306.

[25] R. Cr, S. PS, O. Manaf, S. PP, A. Sujith, Nanochitosan enriched poly ε-caprolactone electrospun wound dressing membranes: A fine-tuning of physicochemical properties, hemocompatibility and curcumin release profile, Int. J. Biol. Macromol. 108 (2018) 1261–1272.

[26] L. Mohammadzadeh, R. Rahbarghazi, R. Salehi, M. Mahkam, A novel eggshell membrane based hybrid nanofibrous scaffold for cutaneous tissue engineering, J. Biol. Eng. (2019) 13.

[27] S. Park, K.S. Choi, D. Lee, D. Kim, K.T. Lim, K.H. Lee, H. Seonwoo, J. Kim, Eggshell membrane: review and impact on engineering, Biosyst. Eng. 151 (2016) 446–463.

[28] X. Li, Z. Cai, D.U. Ahn, X. Huang, Development of an antibacterial nanobiomaterial for wound-care based on the absorption of AgNPs on the eggshell membrane, Colloids Surf. B 183 (2019), 110449.

[29] K.O. Santos, R.C. Barbosa, J. da Silva Buriti, A.G. Bezerra Junior, W.J.B. de Sousa, S.M.C. de Barros, R.J. de Oliveira, M. Fook, Thermal, chemical, biological and mechanical properties of chitosan films with powder of eggshell membrane for biomedical applications, J. Therm. Anal. Calorim. 136 (2019) 725–735.

[30] A.J. Hassiba, M.E. El Zowalaty, T.J. Webster, A.M. Abdullah, G.K. Nasrallah, K. A. Khalil, A.S. Luyt, A.A. Elzatahry, Synthesis, characterization, and antimicrobial properties of novel double-layer nanocomposite electrospun fibers for wound dressing applications, Int. J. Nanomed. 12 (2017) 2205–2213.

[31] H. Adeli, M.T. Khorasani, M. Parvazinia, Wound dressing based on electrospun PVA/chitosan/starch nanofibrous mats: fabrication, antibacterial and cytocompatibility evaluation and in vitro healing assay, Int. J. Biol. Macromol. 122 (2019) 238–254.
[32] S. Alippilakkotte, S. Kumar, L. Sreejith, Fabrication of PLA/Ag nanofibers by green synthesis method using *Momordica charantia* fruit extract for wound dressing applications, Colloids Surf. A 529 (2017) 771–782.
[33] R. Shi, H. Geng, M. Gong, J. Ye, C. Wu, X. Hu, L. Zhang, Long-acting and broad-spectrum antimicrobial electrospun poly (ε-caprolactone)/gelatin micro/nanofibers for wound dressing, J. Colloid Interface Sci. 509 (2018) 275–284.
[34] P. Sathishkumar, Z. Li, B. Huang, X. Guo, Q. Zhan, C. Wang, F.L. Gu, Understanding the surface functionalization of myricetin-mediated gold nanoparticles: experimental and theoretical approaches, Appl. Surf. Sci. 493 (2019) 634–644.
[35] P. Sathishkumar, Z. Li, R. Govindan, R. Jayakumar, C. Wang, F.L. Gu, Zinc oxide-quercetin nanocomposite as a smart nano-drug delivery system: Molecular-level interaction studies, Appl. Surf. Sci. 536 (2021), 147741.
[36] J. Choi, B. Pant, C. Lee, M. Park, S.J. Park, H.Y. Kim, Preparation and characterization of eggshell membrane/PVA hydrogel via electron beam irradiation technique, J. Ind. Eng. Chem. 47 (2017) 41–45.
[37] S. Park, K.S. Choi, W. Kim, D. Lee, D. Kim, M.S. Kim, K. Kim, J. Kim, Engineering nanowrinkled microfibers composed of eggshell membrane and grapheme, Mater. Lett. 229 (2018) 78–81.
[38] M. Baláž, Eggshell membrane biomaterial as a platform for applications in materials science, Acta Biomater. 10 (2014) 3827–3843.
[39] S. Shafiei, M. Omidi, F. Nasehi, H. Golzar, D. Mohammadrezaei, M. Rezai Rad, A. Khojasteh, Egg shell-derived calcium phosphate/carbon dot nanofibrous scaffolds for bone tissue engineering: fabrication and characterization, Mater. Sci. Eng. C 100 (2019) 564–575.
[40] V. Trakoolwannachai, P. Kheolamai, S. Ummartyotin, Characterization of hydroxyapatite from eggshell waste and polycaprolactone (PCL) composite for scaffold material, Compos. Part B Eng. 173 (2019), 106974.
[41] B. Komur, F. Bayrak, N. Ekren, M.S. Eroglu, F.N. Oktar, Z.A. Sinirlioglu, S. Yucel, O. Guler, O. Gunduz, Starch/PCL composite nanofibers by co-axial electrospinning technique for biomedical applications, Biomed. Eng. Online 16 (2017) 40.
[42] J. Li, D. Zhai, F. Lv, Q. Yu, H. Ma, J. Yin, Z. Yi, M. Liu, J. Chang, C. Wu, Preparation of copper-containing bioactive glass/eggshell membrane nanocomposites for improving angiogenesis, antibacterial activity and wound healing, Acta Biomater. 36 (2016) 254–266.
[43] P. Guha Ray, P. Pal, P.K. Srivas, P. Basak, S. Roy, S. Dhara, Surface modification of eggshell membrane with electrospun chitosan/polycaprolactone nanofibers for enhanced dermal wound healing, ACS Appl. Bio Mater. 1 (2018) 985–998.